Desalination and Water Treatment
www.deswater.com

doi: 10.5004/dwt.2021.26797

215 (2021) 90–97
March

Simulation and optimization of mineralization of urine by electrooxidation process using artificial neural network and genetic algorithm

Victor Ruan Silva Nascimento[a], Ataíde Matheus Gualberto dos Santos[b], Josan Carvalho de Figueiredo Filho[b], Eliane Bezerra Cavalcanti[a,b], Manuela Souza Leite[a,b,*]

[a]*Instituto de Tecnologia e Pesquisa, Pós-Graduação em Engenharia de Processos, Av. Murilo Dantas, 300, Prédio do ITP, 49032-040, Aracaju–Sergipe, Brazil, Tel./Fax: +55 79 3218 2190; emails: sl.manuela@gmail.com (M.S. Leite), vitoruan2000@hotmail.com (V.R.S. Nascimento), ebcavalcanti@gmail.com (E.B. Cavalcanti)*

[b]*Universidade Tiradentes, Av. Murilo Dantas, 300, 49032-040, Aracaju–Sergipe, Brazil, Tel./Fax: +55 79 3218 2118, emails: ataidemateus@souunit.com.br (A.M.G. Santos), josancarvalho@gmail.com (J.C.F. Filho)*

Received 14 January 2020; Accepted 6 November 2020

ABSTRACT

Urine can be considered as a special type of effluent; it has a complex composition and high organic load. In recent years the need for improvements in the treatment of human waste has increased, for this reason, electrochemical oxidation is a practical and versatile technique to estimate urine degradation and aid in traditional methods of domestic wastewater treatment. This work aims to use artificial neural networks (ANN) to model urine mineralization kinetics through the electrochemical oxidation process under the influence of the main parameters such as current density (20, 60 and 100 mA cm^{-2}), initial concentration of the dissolved organic carbon (DOC) (1.75, 12.22 and 22.7 g L^{-1}) and reaction time (0 to 480 min). A three-layer neural network with 9 neurons was used in the hidden layer, where a score of mean squared error = 0.0021 and mean absolute error = 0.0345 was obtained. The coupled ANN model and the genetic algorithm was used to find the best operational conditions: Percentage of normalized DOC (above 90%) at a current density of 89 mA cm^{-2}, $[DOC]_0$ of approximately 2.35 g L^{-1} and reaction time of 3.9 h.

Keywords: Artificial intelligence; Urine mineralization; Anodic electrochemical oxidation; Modelling; Wastewater treatment

1. Introduction

World population growth and rapid urbanization have increased the burden of domestic wastewater every day. One of the problems faced due to these factors is water scarcity, an increasingly common reality in many countries [1]. In an attempt to combat or reverse this situation, the interest in the treatment of domestic effluents for reuse has increased. In the composition of household waste, there are particulate or dissolved materials, various organic compounds and microorganisms.

The entire volume of these effluents is directed to water bodies such as rivers, seas and lakes, so efficient and appropriate treatment is required to minimize environmental impact. Many domestic effluents have a high organic load, which causes an increase in biological oxygen demand and a consequent decrease in available oxygen in the water for fish and other aquatic beings. In addition, substances such as phosphorus and nitrogen cause algal blooms that also affect the local ecosystem [2].

Urine can be considered as a special type of organic-laden household effluent. Within its complex composition, the organic fraction contains various substances such as salts, proteins, hormones, etc, [3,4].

Advanced oxidative processes (AOP) have been successfully used for the mineralization of recalcitrant organic pollutants. This technology uses radicals to destroy complex

* Corresponding author.

molecules of organic compounds and reduce them to carbon dioxide, water and inorganic salts [5]. The main radical produced is the hydroxyl radical (•OH) with the second-highest has known oxidation potential of approximately 2.8 V/SHE [6,7]. In addition to this radical, different chain reactions occur during the process with the formation of peroxides and other oxidizing agents (Eqs. (1)–(3)).

$$^{\bullet}OH + RX \rightarrow RX^{+\bullet} + OH^{-} \quad (1)$$

$$^{\bullet}OH + RH \rightarrow R^{\bullet} + H_2O \quad (2)$$

$$^{\bullet}OH + PhX \rightarrow PhX(OH)^{\bullet} \quad (3)$$

Among the AOP, electrochemical oxidation (EO) is an estimated technique for the degradation of urine achieving a higher depletion of chemical oxygen demand and dissolved organic carbon (DOC), and complete deactivation of microorganisms [8]. In recent years the EO application for the complete destruction of several pollutants has been growing [9–12], due to characteristics such as efficiency in large concentration ranges, no generation of toxic intermediate components, easy automation, etc.

Due to the multicomponent character of urine and the complexity of the equations that govern advanced oxidation processes, it is necessary to use techniques that assist in the study of the behavior of processes involving electrochemical oxidation or urine as effluent. More robust models are fundamental to deal with the nonlinearities inherent to the process, which is why the empirical-deterministic approach has gained prominence in the simulation and optimization of effluent degradation processes [13].

Artificial neural networks (ANN) are an excellent alternative to simulate complex and nonlinear systems [14–18] because they do not need the mathematical description of the process phenomenon [19]. ANN is an artificial intelligence technique considered a universal approximator, resulting from its self-learning, fault tolerance and adaptability properties [18–23]. An ANN is an analogy to the functioning of the human brain, with multiple processing units (artificial neurons) distributed in parallel interconnected layers [24,25]. Each connection between two artificial neurons is associated with a weight, represented by vector/matrix [25]. Because it is an empirical model, it can adapt to the particularities of the problem under study, provided there is sufficient experimental information in different process conditions [26].

Simulating the behavior of a process is essential for its large-scale deployment. ANN can be employed to address this need. However, besides knowing the behavior of the process in the face of changing operating conditions, it is of interest to find optimal parameters to maximize its efficiency. Thus, many studies have employed evolutionary algorithms to find the best results produced by trained ANN. The genetic algorithm (GA) is a search program inspired by the principles of natural selection, where the most capable individual survives and transfers his characteristics (information) to future generations [25,27]. In GA the individual represents a possible answer to the problem, each individual is submitted to processes of reproduction (crossover) and mutation in an attempt to produce the best possible answer (optimization).

In this paper, we intend to present the ANN and the genetic algorithm as alternatives for the analysis of the model urine mineralization process through electrochemical oxidation. To simulate the urine electrooxidation process the operating parameters (current density, $[DOC]_0$ and reaction time) were used as ANN inputs and the mineralization kinetic was the output of the neural model. The importance of each entry was assessed in relation to the response by the Garson method. The genetic algorithm was used to search the universe of answers obtained by ANN to find the optimal values for the operational parameters, aiming to maximize the process efficiency.

2. Materials and methods

To perform the experiments initially a model urine solution was prepared to simulate the real effluent [28]. The following reagents were used: urea P.A., Quimex (Brazil); 99% uric acid Sigma-Aldrich (German); creatinine 99% Neon (Brazil); tribal sodium citrate P.A. Vetec (Brazil); sodium chloride P.A. Neon (Brazil); potassium chloride P.A.-ACS Dynamic (German); ammonium chloride P.A. Synth; calcium chloride P.A. Synth; magnesium sulfate P.A.-ACS Synth; sodium bicarbonate P.A.-ACS Synth; sodium oxalate P.A. Neon (Brazil); sodium sulfate P.A. Dynamics (German); nuclear P.A. monophasic sodium phosphate; biphasic sodium phosphate P.A. Nuclear. The proportions used are described in Table 1.

To determine the model urine mineralization, the dissolved organic carbon values were obtained using Shimadzu TOC-LCPH equipment (USA). The obtained data were then used to estimate the DOC removal rate and consequently the mineralization kinetics of the compounds present in model urine.

According to Gozzi et al. [29], for solutions that present several organic compounds, such as the studied urine solution, it is necessary to multiply the number of electrons of each compound by their respective molar fraction, according to Eq. (4). In the mineralization process, 9 electrons for urea, 22 electrons for uric acid, 28 for creatinine and 18 for trisodium citrate, according to reactions from (I) to (IV).

$$n = 9x_{\text{ureia}} + 22x_{\text{ácido úrico}} + 28x_{\text{creatina}} + 18x_{\text{Citrato Trisódio}} + 92x_{\text{Estradiol}} \quad (4)$$

$$CH_4N_2O + 4H_2O \rightarrow CO_2 + NO_3^- + NH_4^+ + 8H^+ + 9e^- \quad (I)$$

$$C_5H_4N_4O_3 + 3H_2O \rightarrow 5CO_2 + 2NO_3^- + 2NH_4^+ + 22H^+ + 22e^- \quad (II)$$

$$C_4H_9N_3O_2 + 12H_2O \rightarrow 4CO_2 + 2NO_3^- + 2NH_4^+ + 29H^+ + 28e^- \quad (III)$$

$$C_6H_5Na_3O_7 + 5H_2O \rightarrow 6CO_2 + 3Na^+ + 15H^+ + 18e^- \quad (IV)$$

2.1. Model solution and electrochemical treatment of urine

The model urine solution was divided into three categories according to their $[DOC]_0$. The first called

Table 1
Composition of synthetic urine

Substance	Chemical formula	Concentration (mol L^{-1})
Urea	CH_4N_2O	0.2000
Sodium chloride	NaCl	0.0540
Potassium chloride	KCl	0.0300
Ammonium chloride	NH_4Cl	0.0150
Sodium sulfate	Na_2SO_4	0.0090
Trisodium citrate	$C_6H_5Na_3O_7$	0.0050
Creatinine	$C_4H_7N_3$	0.0040
Monosodium phosphate	H_2NaO_4	0.0036
Calcium chloride	$CaCl_2$	0.0030
Magnesium sulphate	$MgSO_4$	0.0020
Sodium bicarbonate	$NaHCO_3$	0.0020
Uric acid	$C_5H_4N_4O_3$	0.0010
Disodium phosphate	HNa_2O_4	0.0004
Sodium oxalate	C_2Na_2O	0.0001

concentrated urine, simulates the actual urine concentration without any dilution of the solution components. The second represents the dilution of urine after flushing a domestic toilet. A third, called intermediate, was used as a median of the other concentrations.

For electrochemical oxidation, a boron-doped diamond anode (BDD) and a steel cathode were used as electrodes. During the experiments, three current densities were analyzed: 20, 60 and 100 mA cm^{-2}. For each experiment, varying urine concentration or current density, the samples were collected to quantify dissolved organic carbon at times 0, 5, 15 and 30 min, and after this period a sample was collected at every hour until 8 h reaction time. The collected samples were diluted in ultrapure water at a ratio of 1:20 before DOC analysis.

2.2. Neural model

For the development of the neural model was used the Anaconda package, using the features of Spyder 3.6 software in Python language. The neural network was programmed with random initialization of weights and bias to avoid random initial correlation. The data obtained from the experiments were used to represent the electrochemical degradation of urine. Of the experiment's total (199 data points), 70% of the data were reserved for neural network training, 15% for the validation set and 15% for the test set [29].

The parameters of current density, $[DOC]_0$ and reaction time were used as ANN inputs and removal of normalized DOC (Eq. (5)) as model output. These variables were considered to evaluate the process kinetically and the ranges of these variables are described in Table 2.

$$\text{Removal of normalized DOC} = \frac{\text{DOC}_{\text{final}}}{\text{DOC}_{\text{initial}}} = \frac{\text{DOC}}{\text{DOC}_0} \tag{5}$$

For the modeling of the urine electrochemical oxidation process, a multi-layer perceptron (MLP) back-propagation

Table 2
Operating ranges of the main parameters analyzed

Variable	Range
$[DOC]_0$ (g L^{-1})	1.75–22.7
Current density (mA cm^{-2})	20–100
Reaction time (min)	0–480

neural network was created, consisting of three different layers of artificial neurons. In the input layer, the number of neurons equals the number of input variables, just as in the output layer the number of neurons equals the number of output variables of the model. Between these layers is an intermediate (hidden) layer whose neurons are responsible for processing information (Fig. 1). Each neuron in the hidden layer connects to the neurons in the other layers by a vector product between the information contained in the neuron and a weight representing the binding strength [25]. This relationship is described in Eq. (6).

$$Y_i = \phi\left(\sum_{i=1}^{M} W_i X_i + b\right) \tag{6}$$

where Y_i and X_i are the output and input data of the neuron respectively, ϕ is the transfer function, M represents the number of input data, W_i the neuron weights and b the value of bias.

To define the best ANN architecture, training with different combinations of activation functions was performed for both the hidden and output layers (Table 3), as well as different training algorithms: Adam [30], Adagrad [31] and stochastic gradient descent. For this purpose, the number of hidden neurons, the mean squared error (MSE) and the correlation coefficient (R^2), described in Eqs. (7) and (8), were used as a selection criterion.

$$\text{MSE} = \frac{1}{n}\sum_{i=1}^{n}\left(Y_{\text{exp}} - Y_{\text{cal}}\right)^2 \tag{7}$$

$$R^2 = 1 - \sum_{\text{i=1}}^{n}\left(\frac{\left(Y_{\text{cal}} - Y_{\text{exp}}\right)^2}{\left(Y_{\text{cal}} - Y_m\right)^2}\right) \tag{8}$$

where n represents the number of data, Y_{exp} is the experimental outputs, Y_{cal} is the output calculated by the model and Y_m is the average output value.

Once the architecture of ANN has been defined, new tests have been done to define the number of neurons in the hidden layer. The number of neurons was selected using as performance index the root mean square error (RMSE), mean absolute error (MAE), and mean absolute percentage error (MAPE) described in Eqs. (9)–(11). After this test, the optimized neural network obtained with the best combination of transfer functions, Training algorithm and number of occult neurons was used to predict the mineralization kinetic. All tests were repeated at least 10 times to ensure the representativeness of the data obtained.

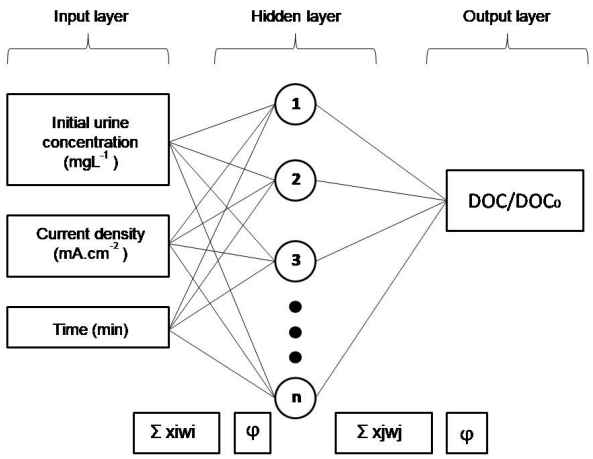

Fig. 1. Representation of a three-layer multilayer perceptron network.

Table 3
Algorithms of transfer functions used to select neural network architecture

Transfer function	Algorithm
Linear – 'linear'	linear(x) = x
Hyperbolic tangent – 'tanh'	tansig(x) = 2(1 + exp(–2x)) – 1
Rectified linear unit – 'relu'	relu(x) = max(x,0)

$$\mathrm{RMSE} = \left[\frac{1}{n}\sum_{i=1}^{n}\left(Y_{\mathrm{exp}} - Y_{\mathrm{cal}}\right)^2\right]^2 \quad (9)$$

$$\mathrm{MAE} = \frac{1}{n}\sum_{i=1}^{n}\left|Y_{\mathrm{exp}} - Y_{\mathrm{cal}}\right| \quad (10)$$

$$\mathrm{MAPE} = \frac{\sum_{i=1}^{n}\frac{Y_{\mathrm{exp}} - Y_{\mathrm{cal}}}{Y_{\mathrm{exp}}}}{n} \quad (11)$$

In order to optimize the operational parameters under analysis ($[DOC]_0$, applied current density and reaction time) the genetic algorithm selected individuals as a set of neural model inputs. The predicted ANN response was evaluated and a new population was generated based on these responses (Fig. 2). For the construction of GA, the configurations elucidated in Table 4 were used.

The restrictions for searching the genetic algorithm were established according to the experimental conditions used for data acquisition. The current density limit was 100 mA cm^{-2}, the maximum time of 8 h, $[DOC]_0$ of 1.75 g L^{-1} and the maximum number of generations equal to 100.

3. Results and discussions

As previously mentioned, the database used for the development of the models (ANN_AG) was obtained from the evolution of the electrooxidation reaction (monitoring of the removal of normalized DOC) under different experimental conditions of $[DOC]_0$ and current density. Replicates were performed to allow evaluating the reproducibility of the process (Fig. 3). An experimental error of removal of normalized DOC of 13.72% was determined, within an acceptable margin of error.

Different ANN was developed for predicting mineralization kinetic. Table 5 shows the results of ANN architecture optimization tests with different transfer functions and training algorithms.

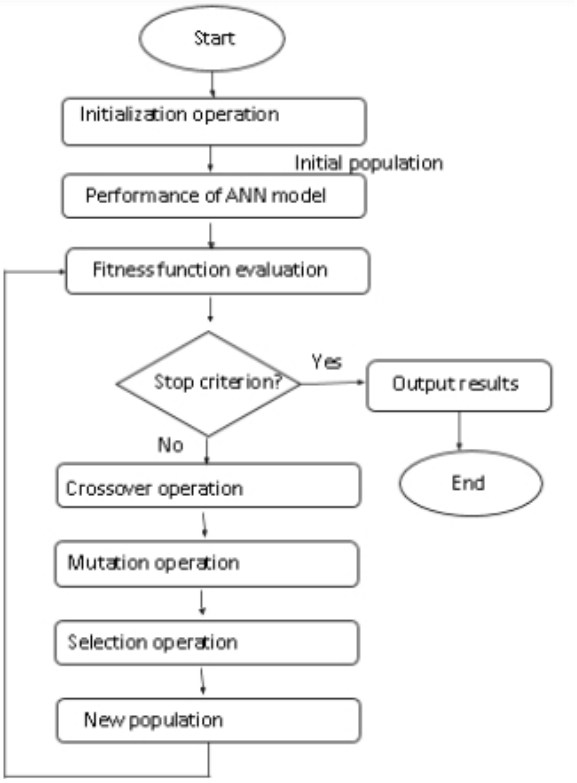

Fig. 2. Flowchart of optimization electrooxidation process based on artificial neural network and genetic algorithm.

Table 4
Genetic algorithm parameters used to optimize operating conditions

Settings	Genetic algorithm
Number of variables	3
Population type	Double vector
Population size	25
Scale function	Rank
Selection function	Stochastic
Elitism	2 individuals
Crossover rate	80%
Mutation rate	5%
Number of generations	100
Fitness function	Trained artificial neural network

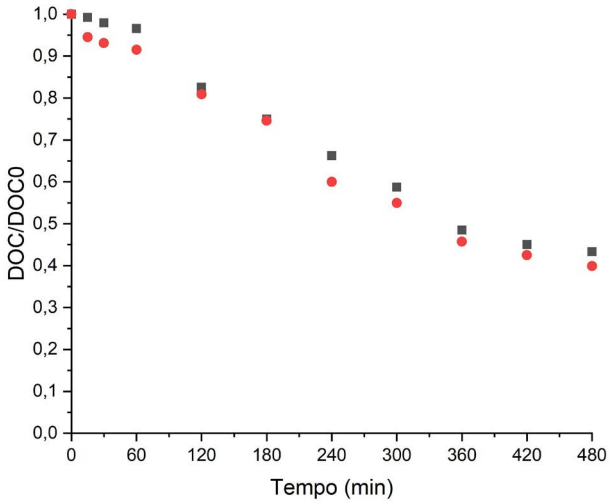

Fig. 3. Evaluation of data reproducibility.

In Table 5 it can be observed that the Adam algorithm [30] stands out against the other training algorithms for the prediction of synthetic urine electrochemical oxidation data. The best-suited transfer functions were the hyperbolic tangent between the input layer and the hidden layer, and the linear function between the hidden layer and the output layer. The choice of architecture is based on the responses of a low MSE value (0.0079) and a correlation coefficient capable of representing 91.63% of the experimental data.

The parameters obtained in the definition of the ANN architecture varied the number of neurons in the hidden layer from 3 to 20 neurons. The performance model was evaluated (Fig. 4) under the statistical RMSE, MAE, and MAPE values.

Fig. 4 shows higher error values in the first neurons, with the addition of new neurons in the occult layer gradually decreases the error until the 9th neuron. Inserting additional neurons after this condition increases the error value again, which could unnecessarily increase the complexity of the model and result in overfitting [32]. For this reason, the topology chosen for the database has 3 input layer neurons, 9 hidden layer neurons and 1 output layer neuron (3:9:1).

Results achieved for MSE and MAE were 0.0021 and 0.0345, respectively, from the architecture parameters shown in Table 6. Both performance indices presented values lower the calculated experimental error (Eq. (12)) equal to 0.1372. Fig. 5 shows the correlation between the simulated outputs by the network and the experimental responses. If the points are close to a straight line it means there is a strong correlation and a low prediction error [19,21,26].

$$\text{Error} = \sum_{i=1}^{n} \frac{Y_{\text{exp}} - Y_{\text{cal}}}{Y_{\text{exp}}} \tag{12}$$

The proximity of the identity line to the points on the graph (Fig. 5) reflects the successful generalization of mineralization kinetics during electrochemical oxidation of synthetic urine, denoting the ability to predict process performance under different operating conditions.

Table 5
Summary of test results for the optimization of artificial neural network architecture

Training algorithm	Hidden layer function	Output layer function	Mean squared error	R^2
	relu	relu	0.0379	0.6350
	relu	tanh	0.0260	0.6571
	relu	selu	0.0279	0.4306
	tanh	selu	0.0212	0.7936
Adam	tanh	linear	0.0079	0.9163
	tanh	relu	0.0191	0.8926
	linear	linear	0.0255	0.5797
	linear	selu	0.0398	0.6251
	linear	tanh	0.0188	0.7773
	relu	relu	0.1611	–0.4711
	relu	tanh	0.0929	0.1350
	relu	selu	0.1079	0.0292
	tanh	tanh	0.0455	0.3244
Adagrad	tanh	linear	0.0604	0.5158
	tanh	relu	0.0533	0.4775
	linear	linear	0.1045	–0.3962
	linear	selu	0.0867	0.0480
	linear	tanh	0.1427	–0.3087
	relu	relu	0.0810	0.3682
	relu	selu	0.0717	0.3338
	relu	linear	0.0410	0.6893
Stochastic	tanh	tanh	0.0382	0.4637
gradient	tanh	selu	0.0139	0.6936
descent	tanh	linear	0.0231	0.7041
	linear	linear	0.0434	0.5693
	linear	selu	0.0510	0.4894
	linear	tanh	0.0572	0.4082

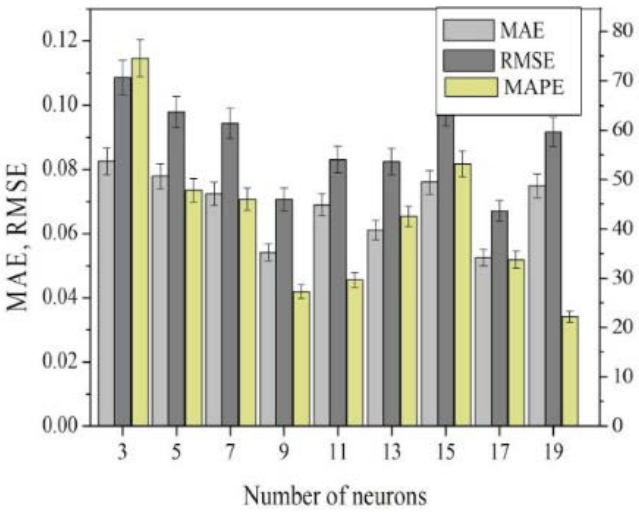

Fig. 4. Selection of model artificial neural network from statistical indexes.

Table 6
Topology and architecture parameters selected for the artificial neural network

Settings	Artificial neural network
Number of inputs	3
Number of outputs	1
Number of hidden neurons	9
Transfer functions	tanh, linear
Training algorithm	Adam

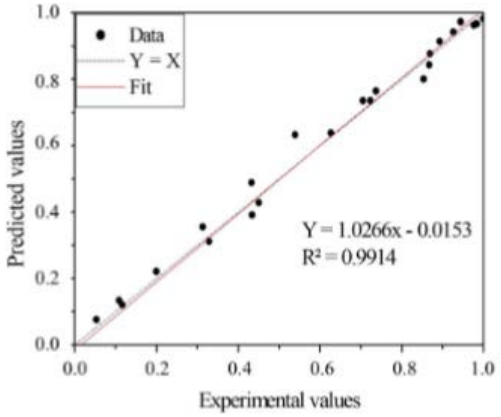

Fig. 5. Experimental vs. predicted using the optimized multilayer perceptron network.

In studies of electrochemical treatment of pollutants, it is essential to try to reproduce the reaction in conditions closer to the actual effluent. This criterion helps to ensure that the results found can be reproduced on a larger scale. Thus, all tests were performed at room temperature, so that during the experiments no chemical additive was used as a supporting electrolyte, since the urine solution itself contains inorganic ions, making electrooxidation possible in real conditions [4,28,33].

The salts present in the solution, in addition to contributing to conductivity, also contributed to the formation of secondary oxidants (Eqs. (V)–(X)), increasing the efficiency of the process [34]. Under these conditions, non-linearities about the process are common, due to the complexity of the matrix, diversity of electrolytes and organic compounds present in solution, the formation of intermediates and the performance of secondary oxidants.

$$2Cl^- \rightarrow Cl_2 + e^- \quad (V)$$

$$Cl_2 + H_2O \rightarrow HClO + Cl^- + H^+ \quad (VI)$$

$$HClO \leftrightarrow H^+ + ClO^- \quad (VII)$$

$$2SO_4^{2-} \rightarrow S_2O_8^{2-} + 2e^- \quad (VIII)$$

$$2PO_4^{3-} \rightarrow P_2O_8^{2-} + 4e^- \quad (IX)$$

$$2CO_3^{2-} \rightarrow C_2O_6^{2-} + 2e^- \quad (X)$$

These oxidizing species contribute to the degradation of organic compounds, together with the radical •OH, as they attack the bonds of organic molecules promoting the formation of smaller chain by-products. These secondary oxidants are also one of the main responsible for the non-linearities that occur during the mineralization process of organic compounds. The main factor for the formation of oxidizing species is the current density applied, therefore, this is one of the most relevant parameters for electrochemical oxidation. Fig. 6 shows the accuracy of the neural model developed for the simulation of urine mineralization behavior under different current densities and intermediate concentrations (12.22 g L^{-1}).

It should be noted that the developed neural model was able to simulate the urine mineralization process under different operational conditions. As seen in the profile presented in Fig. 6, despite the multicomponent character of the matrix and the simultaneous influence of all secondary reactions, the neural model was able to accurately predict mineralization kinetics.

The Garson method (Eq. (13)) was used to calculate the relative importance of operating variables from the matrix of synaptic weights and bias generated by ANN. This equation can account for the individual contributions of each independent variable in the final answer.

$$I_j = \frac{\sum_{m=1}^{m=N_h}\left[\left(\frac{\left|W_{jm}^{ih}\right|}{\sum_{k=1}^{N_i}\left|W_{km}^{ih}\right|}\right)\times\left|W_{mn}^{ho}\right|\right]}{\sum_{k=1}^{k=N_i}\left[\sum_{m=1}^{m=N_h}\left(\frac{\left|W_{jm}^{ih}\right|}{\sum_{k=1}^{N_i}\left|W_{km}^{ih}\right|}\right)\times\left|W_{mn}^{ho}\right|\right]} \quad (13)$$

where I_j is the relative importance of the input variable in the output variable; N_i and N_h are the numbers of input and hidden neurons, respectively; W is the synaptic weight of the connections between the neural network layers; '*i*', '*h*' and '*o*' refer to the input, hidden and output layers respectively; '*k*', '*m*' and '*n*' refer to the number of input, hidden and output neurons, respectively.

From the Garson test (Table 7) all variables have a major contribution to the process. It follows from this that no variable could be neglected in the analysis of synthetic urine mineralization.

The coupled ANN model and genetic algorithm to predict the performance of the electrooxidation process used for urine treatment can be useful for scale-up. The goal of GA optimization was to find the maximum efficiency of DOC removal from urine. The generated individuals represent the combination of the three input variables of the model. Each optimal condition was evaluated according to the ANN response (fitness function). The optimal values for maximum urine mineralization found by GA were: current density of 89 mA cm^{-2}, $[DOC]_0$ of approximately 2.35 g L^{-1} and reaction time of 3.9 h, resulting in removal efficiency of

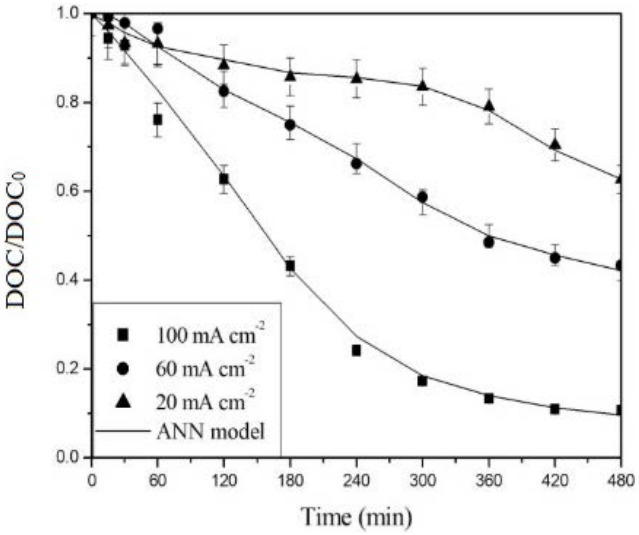

Fig. 6. Normalized mineralization decay: current (20, 60 and 100 mA cm^{-2}), $[DOC]_0$ (12.23 g L^{-1}) using the optimized multi-layer perceptron network.

Table 7
Results of relative importance of model inputs from the Garson equation

Inputs	Relative importance
Current density	31.28%
$[DOC]_0$	30.55%
Reaction time	38.17%

total organic carbon (TOC) around 91%, close to that found by other authors who used electrooxidation for degradation of organic compounds [33,34]. Steter et al. [33] studied the electrooxidation process with electrogenerated H_2O_2 on site for removal of methylparaben using a BDD at a current of 66.7 mA cm^2 and reached a mineralization efficiency of 89%. In another study, Murugananthan et al. [34] applied this process for the mineralization of the hormone 17b-estradiol, under a current of 50 mA cm^2, and reached 94% mineralization efficiency. It is important to note that the initial TOC values of the studies by Steter et al. [33] and Murugananthan et al. [34] are much smaller (100 and 0.39 ppm, respectively) than the initial DOC value of the multicomponent synthetic urine solution used in our study (3,600 ppm). The results found in the work indicate that electrooxidation could be an effective alternative technique for the treatment of urine present in domestic wastewater treatment.

4. Conclusions

In this paper, we developed an empirical deterministic model using ANN to predict the efficiency electrochemical mineralization of urine as domestic effluent. A classical ANN-based model was used, the MLP neural network, with 3:9:1 topology, Adam algorithm [30] and transfer functions hyperbolic tangent and the linear function for the hidden and output layers, respectively. This configuration provides satisfactory model performance indices with low prediction errors and a high correlation index between predicted and experimental data (MSE of 0.0021, MAE of 0.0345 and R^2 of 0.9914). The optimization genetic algorithm indicated a maximum urine percentage of normalized removal of 91% at 3.9 h reaction time, 89 mA cm^{-2} current density and $[DOC]_0$ of 2.35 g L^{-1}. This studied might contribute to the industrial application of neural networks and genetic algorithms for monitoring and developing control strategies of the wastewater treatment process.

Acknowledgment

This research was supported by CAPES (Coordination for the Improvement of Higher Education Personnel) under financing code 001, FAPITEC/SE (Foundation of Support to Research and Technological Innovation of the State of Sergipe), FINEP (Financier of Studies and Projects, grant number: 564584/2020) and CNPq (National Council for Scientific and Technological Development; grant number: 420717/2018-8).

References

[1] M.N. Chong, B. Jin, C.W.K. Chow, C. Saint, Recent developments in photocatalytic water treatment technology: a review, Water Res., 44 (2010) 2997–3027.
[2] A. Khataee, A. Fazli, M. Fathinia, F. Vafaei, Simultaneous elimination of two species of algae from a contaminated water through ozonation process: mechanism and destruction intermediates, Ozone Sci. Eng., 41 (2019) 35–45.
[3] S.D. Lu, H.N. Li, G.C. Tan, F. Wen, M.T. Flynn, X.P. Zhu, Resource recovery microbial fuel cells for urine-containing wastewater treatment without external energy consumption, Chem. Eng. J., 373 (2019) 1072–1080.
[4] A. Schranck, R. Marks, E. Yates, K. Doudrick, Effect of urine compounds on the electrochemical oxidation of urea using a nickel cobaltite catalyst: an electroanalytical and spectroscopic investigation, Environ. Sci. Technol., 52 (2018) 8638–8648.
[5] A.J. Kedir, B. Tawabini, A. Al-Shaibani, A.A. Bukhari, Treatment of water contaminated with methyl tertiary butyl ether using UV/chlorine advanced oxidation process, Desal. Water Treat., 57 (2016) 19939–19945.
[6] F.C. Moreira, R.A.R. Boaventura, E. Brillas, V.J.P. Vilar, Electrochemical advanced oxidation processes: a review on their application to synthetic and real wastewaters, Appl. Catal., B, 202 (2017) 217–261.
[7] P.V. Nidheesh, M.H. Zhou, M.A. Oturan, An overview on the removal of synthetic dyes from water by electrochemical advanced oxidation processes, Chemosphere, 197 (2018) 210–227.
[8] S. Dbira, N. Bensalah, A. Bedoui, P. Cañizares, M.A. Rodrigo, Treatment of synthetic urine by electrochemical oxidation using conductive-diamond anodes, Environ. Sci. Pollut. Res., 22 (2015) 6176–6184.
[9] O.T. Can, COD removal from fruit-juice production wastewater by electrooxidation electrocoagulation and electro-Fenton processes, Desal. Water Treat., 52 (2014) 65–73.
[10] R. Dewil, D. Mantzavinos, I. Poulios, M.A. Rodrigo, New perspectives for advanced oxidation processes, J. Environ. Manage. 195 (2017) 93–99.
[11] L. Yu, M. Han, F. He, A review of treating oily wastewater, Arabian J. Chem., 10 (2017) S1913–S1922.
[12] M.A. Oturan, J.-J. Aaron, Advanced oxidation processes in water/wastewater treatment: principles and applications. a review, Crit. Rev. Env. Sci. Technol., 44 (2014) 2577–2641.
[13] D.F. Viana, G.R. Salazar-Banda, M.S. Leite, Electrochemical degradation of Reactive Black 5 with surface response and

artificial neural networks optimization models, Sep. Sci. Technol., 53 (2018) 2647–2661.
[14] G.G. Lenzi, R.F. Evangelista, E.R. Duarte, L.M.S. Colpini, A.C. Fornari, R. Menechini Neto, L.M.M. Jorge, O.A.A. Santos, Photocatalytic degradation of textile reactive dye using artificial neural network modeling approach, Desal. Water Treat., 57 (2016) 14132–14144.
[15] A. Akbarpour, A. Khataee, M. Fathinia, B. Vahid, Development of kinetic models for photoassisted electrochemical process using Ti/RuO_2 anode and carbon nanotube-based O_2-diffusion cathode, Electrochim. Acta, 187 (2016) 300–311.
[16] G.R. Oliveira, A.V. Santos, A.S. Lima, C.M.F. Soares, M.S. Leite, Neural modelling in adsorption column of cholesterol-removal efficiency from milk, LWT-Food Sci. Technol., 64 (2015) 632–638.
[17] M.R. Gadekar, M.M. Ahammed, Coagulation/flocculation process for dye removal using water treatment residuals: modelling through artificial neural networks, Desal. Water Treat., 57 (2016) 26392–26400.
[18] Y.M. da Silva Veloso, M.M. de Almeida, O.L.S. de Alsina, M.S. Leite, Artificial neural network model for the flow regime recognition in the drying of guava pieces in the spouted bed, Chem. Eng. Commun., 207 (2019) 549–558.
[19] Y.M. da Silva Veloso, M.M. de Almeida, O.L.S. de Alsina, M.L. Passos, A.S. Mujumdar, M.S. Leite, Hybrid phenomenological/ANN-PSO modelling of a deformable material in spouted bed drying process, Powder Technol., 366 (2020) 185–196.
[20] O.I. Abiodun, A. Jantan, A.E. Omolara, K.V. Dada, N.A. Mohamed, H. Arshad, State-of-the-art in artificial neural network applications: a survey, Heliyon, 4 (2018) e00938.
[21] V.K. Ojha, A. Abraham, V. Snášel, Metaheuristic design of feedforward neural networks: a review of two decades of research, Eng. Appl. Artif. Intell., 60 (2017) 97–116.
[22] A.R. Khataee, M.B. Kasiri, Artificial neural networks modeling of contaminated water treatment processes by homogeneous and heterogeneous nanocatalysis, J. Mol. Catal. A: Chem, 331 (2010) 86–100.
[23] F. Salehi, S.M.A. Razavi, Modeling of waste brine nanofiltration process using artificial neural network and adaptive neuro-fuzzy inference system, Desal. Water Treat., 57 (2016) 14369–14378.
[24] N. Messikh, M. Chiha, F. Ahmedchekkat, A. Al Bsoul, Application of radial basis function neural network for removal of copper using an emulsion liquid membrane process assisted by ultrasound, Desal. Water Treat., 56 (2015) 399–408.
[25] S. Azadi, A. Karimi-Jashni, S. Javadpour, Modeling and optimization of photocatalytic treatment of landfill leachate using tungsten-doped TiO_2 nano-photocatalysts: application of artificial neural network and genetic algorithm, Process Saf. Environ. Prot., 117 (2018) 267–277.
[26] A. Afram, F. Janabi-Sharifi, A.S. Fung, K. Raahemifar, Artificial neural network (ANN) based model predictive control (MPC) and optimization of HVAC systems: a state of the art review and case study of a residential HVAC system, Energy Build., 141 (2017) 96–113.
[27] A. Picos, J.M. Peralta-Hernández, Genetic algorithm and artificial neural network model for prediction of discoloration dye from an electro-oxidation process in a press-type reactor, Water Sci. Technol., 78 (2018) 925–935.
[28] S. Chutipongtanate, V. Thongboonkerd, Systematic comparisons of artificial urine formulas for in vitro cellular study, Anal. Biochem., 402 (2010) 110–112.
[29] F. Gozzi, I. Sirés, A. Thiam, S.C. de Oliveira, A.M. Junior, E. Brillas, Treatment of single and mixed pesticide formulations by solar photoelectro-Fenton using a flow plant, Chem. Eng. J., 310 (2017) 503–513.
[30] D.P. Kingma, J. Ba, Adam: A Method for Stochastic Optimization, Published as a Conference Paper at the 3rd International Conference for Learning Representations, San Diego, 2015. Available at: http://arxiv.org/abs/1412.6980 (accessed June 14, 2019).
[31] Y. Lu, J. Lund, J. Boyd-Graber, Why ADAGRAD Fails for Online Topic Modeling, Proceedings of the 2017 Conference on Empirical Methods in Natural Language Processing, Association for Computational Linguistics, Copenhagen, Denmark, 2017, pp. 446–451.
[32] L. Das, U. Maity, J.K. Basu, The photocatalytic degradation of carbamazepine and prediction by artificial neural networks, Process Saf. Environ. Prot., 92 (2014) 888–895.
[33] J.R. Steter, E. Brillas, I. Sirés, On the selection of the anode material for the electrochemical removal of methylparaben from different aqueous media, Electrochim. Acta, 222 (2016) 1464–1474.
[34] M. Murugananthan, S. Yoshihara, T. Rakuma, N. Uehara, T. Shirakashi, Electrochemical degradation of 17β-estradiol (E2) at boron-doped diamond (Si/BDD) thin film electrode, Electrochim. Acta, 52 (2007) 3242–3249.